Electronic Supplementary Information

Super-Resolution Fluorescence Nanoscopy Applied to Imaging Core-Shell Photoswitching Nanoparticles and Their Self-Assemblies

Tian, Zhiyuan; Li, Alexander D. Q.; Hu, Dehong

Materials and Methods.

General. Solvents and reagents were purified where necessary using literature methods. Cover glasses (Gold Seal No. 1) were purchased from Fisher. All compounds for monomer and nanoparticle synthesis were purchased from Sigma-Aldrich.

Synthesis of photoswitchable fluorescent polymer nanoparticles: Photoswitchable polymer nanoparticles were synthesized via a radical-initiated microemulsion polymerization with minor modifications.[1] In a typical protocol, 30 g DI water, 0.56 mmol acrylamide and 0.2 mmol acrylic acid were loaded into a 100-mL flask equipped with a magnetic stir bar. Oxygen was purged from the system by bubbling argon gas for 30 minutes. Subsequently, 0.1 g Tween 20 surfactant was added to the solution. The reaction flask was then immersed into 90°C oil bath for 5 minutes following by an injection of 0.02 mmol polymerization initiator, namely 4, 4'-azobis (4-cyano-valeric acid). After another 5 minutes, co-monomer mixture containing 3 mg spiropyran compounds, 0.25 mmol styrene, and 0.15 mmol divinylbenzene (DVB) was syringe-injected while maintaining the reaction temperature and the stirring speed. Polymerization proceeded for another 3.5 hours. The as-prepared polymer nanoparticles were washed with chloroform to remove the unreacted organic reactants. The residual chloroform was then removed from the water phase under reduce pressure, yielding a milky colloidal sample.

Diameter characterization. Dynamic light scattering (DLS) measurements were carried out on a Beckman-Coulter N4 instrument at fixed scattering angles of 62.6° and 90° with the 632.8 line of a He-Ne laser as excitation source; standard polystyrene microspheres were used for instrument calibration. The average particle sizes and size distributions were obtained from the autocorrelation decay functions by CONTIN analysis using standard software package supplied by Beckman-Coulter. A JEOL 1010 transmission electron microscope (TEM) operated at 100 kV was employed to obtain TEM images. The microscope sample was prepared by placing a drop of the polymer dispersion on a carbon-coated Cu grid, followed by solvent evaporation at room temperature.

Nanoparticle Self-Assembly on $CaCl_2$ Surface. Photoswitchable nanoparticles as synthesized above was mixed with 1.00 mM of $CaCl_2$ aqueous solution. The molarity of the nanoparticles was estimated using the feed materials weight and the size of the nanoparticles, which was determined to be ~70 nm for this experiment. The calculated concentration is approximately 1.14 nM. The solution containing both $CaCl_2$ (aq.) and the photoswitchable nanoparticles was casted on a microscope coverslip and water was allowed to evaporate. During the drying process, crystallites of $CaCl_2$ were formed and nanoparticles having

carboxylates on their surfaces self-assembled around the micro-sized crystals as revealed by PULSAR nanoscopy.

PULSAR microscope setup and imaging method: Cover glass samples were placed on the stage of an inverted microscope (Olympus IX81) equipped with a high numerical aperture oil immersion objective (Olympus PLAPO100XO3, 100X, 1.45 NA). Connected to the side port of the microscope was a highly sensitive EMCCD detector (ANDOR Ixon+). Excitation light from the back port of the microscope was redirected by an array of appropriate filter sets into the back aperture of the objective. Emission light was collected through the same objective and directed to the side port where the EMCCD is connected. For wide field super-resolution imaging, a laser beam was first attenuated with neutral density filters before entering the back aperture of the microscope objective to produce wide field illumination. The 375-nm laser (CrystaLaser, DL375-016) and 561-nm laser (CrystaLaser, CL561-075-O) were combined collinearly by a 45º-dichroic beam combiner before sending to the microscope. To obtain PULSAR images, we employed the 375-nm laser at 1-2 ms duration and 0.06-0.7 W/cm^2 to switch a subset of spiropyran molecules into merocyanine dyes. Subsequently, the 561-nm laser was used to image the on-switched merocyanine flurophores at 1-s exposure rate with a power density of 848 W/cm^2. This photoswitching and imaging process was repeated many times to collect enough frames for reconstructing the PULSAR images.

Generality of self-organization of polymer nanoparticles.

Figure S1a and S1b display images from conventional microscopy and PULSAR nanoscopy, respectively. The conventional images have not only lower resolution but also higher background. Figure S1b reveals that observation of rectangle and circular patterns in Figure 1 and 2 in the main text is not isolated events. There are many circular and rectangle patterns in the field of view when zooming out. These facts are confirmed in Figure S1c and S1d. We therefore conclude that polymeric nanoparticles with negative charges on their surfaces preferentially self-organize on $CaCl_2$ solids or crystals.

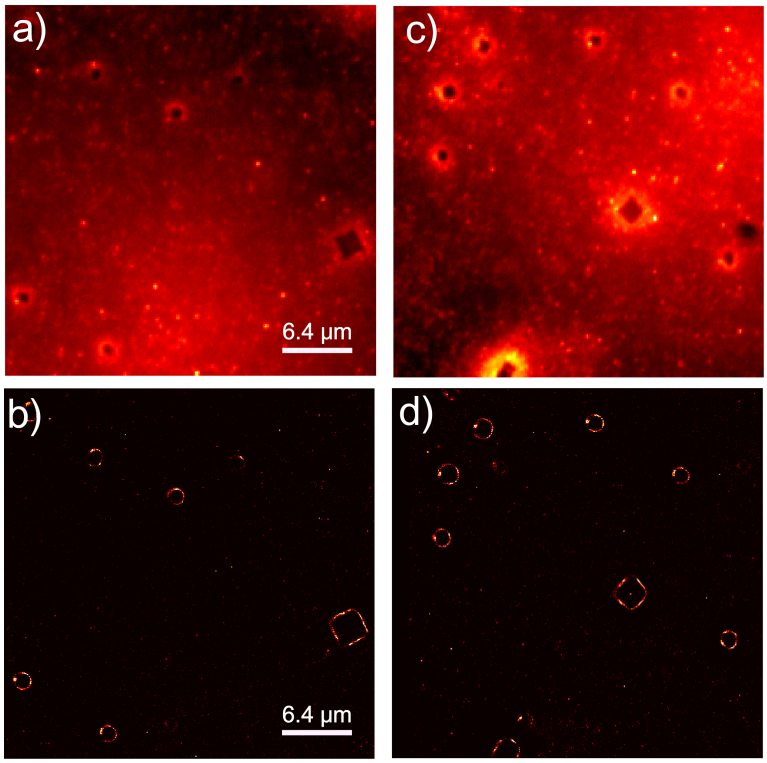

Figure S1. A larger view (32 x 32 μm^2) reveals that rectangle and circular crystallites are quite common in such samples. Image (a) is obtained from conventional microscopy; its corresponding high-resolution PULSAR image of the same area is displayed in (b) after processing 500 single-molecule frames. Images (c) and (d) are similar to images (a) and (b), except in a different area of the same sample.

Negative control of self-organization of polymer nanoparticles.

Nanoparticles having carboxylic groups on their spherical surfaces self-organize around $CaCl_2$ crystals, as discussed in the main text. To verify the template role of $CaCl_2$ in directing the self-assembly of polymer nanoparticles, a negative control test was carried out by allowing the same nanoparticle sample to "self-organize" without the presence of $CaCl_2$. A typical high-resolution image obtained from this control sample yields no circles or rectangles, as shown in Figure S2, in sharp contrast to those shown in Figure S1.

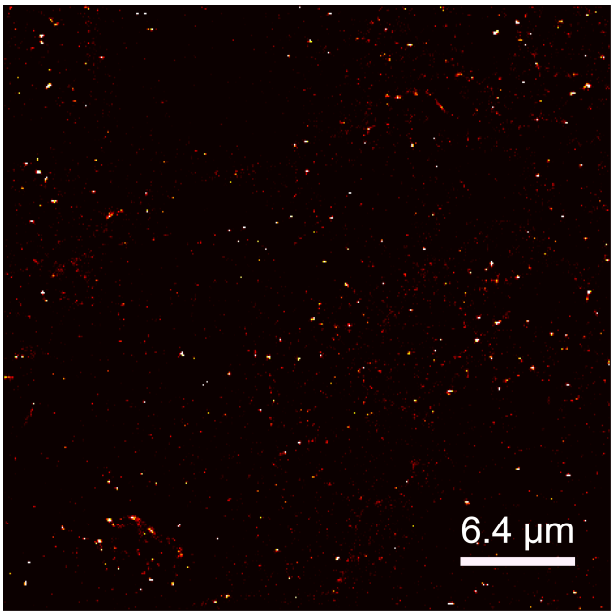

Figure S2. PULSAR picture of the negative control sample. In the absence of $CaCl_2$, no circular or rectangle structures were observed, indicating the important roles that Ca^{2+} ions play during self-organization of nanoparticles.

Controlled interfering fluorophores photobleaching and the subsequent PULSAR imaging.

In our experiment, the background fluorescence was successfully photobleached and suppressed without photobleaching the PULSAR signal-the on-switched signals from the photoswitchable SP-MC pairs. Our photoswitchable nanoparticles and dyes have been developed for cellular imaging even though we used $CaCl_2$ crystal organization strategy here. Single-molecule imaging experiments in cells are extremely difficult, if not impractical. The barrier is autofluorescence background that may overwhelm the single-molecule fluorescence signal. It is sometimes impractical to photobleach autofluorescence using fluorescence excitation irradiation because many standard fluorophores and photoswitchable proteins and photoactivable dyes absorb the excitation energy and will also be photobleached.[2, 3] Our photoswitchable high-resolution probes, however, have unique advantages: the fluorescence-on state absorbs in green-yellow region (570 nm) and fluoresces in the red to near infrared region (NIR: 600-750 nm); importantly, the off-state adopts a spiro-ring and does not absorb in the green-yellow region at all.[4] Such a unique combination of photophysical properties enables pre-photobleaching of background before PULSAR imaging as well as during PULSAR data acquisition; thus autofluorescence background is greatly suppressed. Figure S3 exemplifies one such image. After about one-hour photobleaching by high-power 561-nm laser (848 W/cm^2), the same region shown in Figure S1b were pulsed again with alternating 375-nm on-switching laser and 561-nm imaging laser to yield Figure S3. The interfering fluorescence is greatly reduced, but the photoswitchable spiropyran-merocyanine dyes inside the nanoparticles faithfully reproduced the pattern observed in Figure S1 b. Note that interfering fluorescence is noise from sources other than photoswitchable nanoparticles. Here the non-organized spots are considered signal since they originate from nanoparticles.

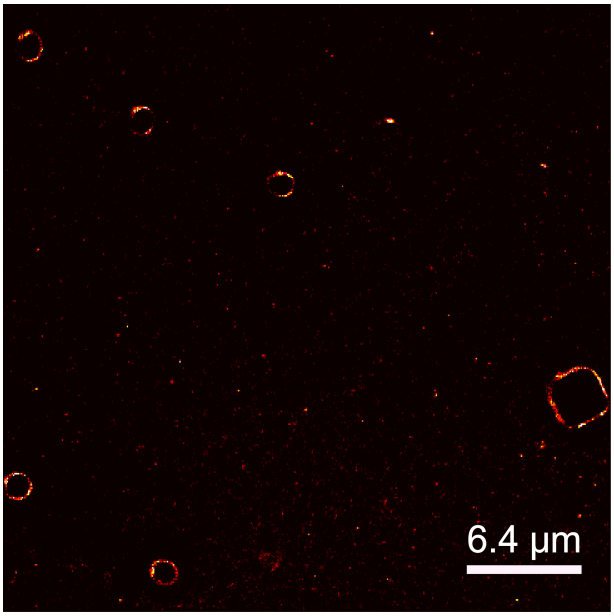

Figure S3. PULSAR picture acquired after extensive illumination by 561-nm laser with the purpose of photobleaching the interfering fluorophores. It is noted that while the 561-nm laser photobleaches the interfering fluorophores, it also photoswitches the merocyanine dyes back to spiropyran molecules for later photoswitching experiments. After extensive photobleaching by 561-nm laser, one can repeat the procedure carried in Figure S1a and readily reproduce the above image (Figure S3) with a slight drift of the microscope. This demonstrates a unique advantage of our photoswitching probes, which allow us to photobleach the interfering fluorophores as much as possible without causing significant damage to spiropyran molecules because they do not absorb at 561 nm.

Reference

1. M. Q. Zhu, L. Y. Zhu, J. J. Han, W. W. Wu, J. K. Hurst, A. D. Q. Li, J. Am. Chem. Soc. 2006, **128**, 4303.
2. C. I. Richards, J. C. Hsiang, D. Senapati, S. Patel, J. H. Yu, T. Vosch, R. M. Dickson, J. Am. Chem. Soc. 2009, **131**, 4619.
3. C. I. Richards, J. C. Hsiang, R. M. Dickson, J. Phys. Chem. B 2010, 114, 660.
4. D. H. Hu, Z. Y. Tian, W. W. Wu, W. Wan, A. D. Q. Li, J. Am. Chem. Soc. 2008, **130**, 15279